



CHORUS

This is the accepted manuscript made available via CHORUS. The article has been published as:

Cavity Cooling of Many Atoms

Mahdi Hosseini, Yiheng Duan, Kristin M. Beck, Yu-Ting Chen, and Vladan Vuletić

Phys. Rev. Lett. **118**, 183601 — Published 1 May 2017

DOI: [10.1103/PhysRevLett.118.183601](https://doi.org/10.1103/PhysRevLett.118.183601)

Cavity cooling of many atoms

Mahdi Hosseini,^{1,*} Yiheng Duan,¹ Kristin M. Beck,^{1,†} Yu-Ting Chen,^{1,2} and Vladan Vuletić¹

¹*Department of Physics and Research Laboratory of Electronics,
Massachusetts Institute of Technology, Cambridge, Massachusetts 02139, USA*

²*Department of Physics, Harvard University, Cambridge, Massachusetts, 02138, USA*

(Dated: March 8, 2017)

We demonstrate cavity cooling of all motional degrees of freedom of an atomic ensemble using light that is far detuned from the atomic transitions by several gigahertz. The cooling is achieved by cavity-induced frequency-dependent asymmetric enhancement of the atomic emission spectrum, thereby extracting thermal kinetic energy from the atomic system. Within 100 ms, the atomic temperature is reduced from 200 μK to 10 μK , where the final temperature is mainly limited by the linewidth of the cavity. In principle, the technique can be applied to molecules and atoms with complex internal energy structure.

The coherent interaction of atoms with an electromagnetic mode of a high-finesse optical resonator can be used to control the electromagnetic field [1–6], or to entangle the internal states of many atoms [7–9]. Moreover, the strong light-matter interaction provided by the optical resonator can be employed to control and cool the external degrees of freedom of atoms or other particles [10–22], as well as massive oscillators [23–29]. Notably, cooling with light far off resonant from any atomic or molecular transition becomes possible, as the sign of the velocity dependent force can be set by the frequency of the cavity, rather than that of the atomic transition [10, 11]. Cavity cooling uses the fact that the spectrum of the light scattered by a moving particle is broadened relative to the incident light, and contains both lower-frequency (Stokes) and higher-frequency (anti-Stokes) components, corresponding to an increase or decrease of the particle’s kinetic energy, respectively. By tuning the cavity to the anti-Stokes sideband, it is then possible to cool moving objects via light scattering into the cavity [14, 30]. To date, cavity cooling has been applied to single atoms [15], ions [16], nanoscale particles [20–22], the center-of-mass mode of an atomic ensemble [17], and nanomechanical oscillators [23–29]. Moreover, a Bose-Einstein condensate has been transferred deterministically between two momentum states via cavity scattering [18].

For a large ensemble in a low-finesse resonator, cooling by collective emission has been observed [19]. While some extensions of the cavity cooling model [13, 31–33] predict the possibility of collectively enhanced cooling, the experimental observations disagreed strongly with the single-atom two-level model of cavity cooling [10, 11, 14]. In particular, in Ref. [19] cooling was only observed at relatively small detuning of ~ 200 MHz from atomic reso-

nance, and tuning the cavity to the anti-Stokes sideband was not required.

In this Letter, we demonstrate simultaneous cavity cooling of all motional degrees of freedom in an ensemble containing a few hundred atoms. The cooling is performed at a large detuning of several gigahertz from atomic resonance. The maximal detuning is only limited by the low available laser power of a few μW . The temperature is reduced by a factor of 20, and the phase space density increased by over two orders of magnitude, within 100 ms. The observations are well described by a simple single-particle model of cavity cooling [14]. The cooling rate is set by the photon scattering rate into the cavity at the given laser power and chosen detuning from atomic resonance, while the final temperature of 10(1) μK is limited by the cavity linewidth κ ($\kappa = 2\pi \times 160$ kHz, $\hbar\kappa/k_B = 7.6$ μK for our system).

Our system consists of an ensemble of ^{133}Cs atoms held within the TEM_{00} mode of a high-finesse optical cavity that enhances both the cooling light (wavelength $\lambda_c = 852$ nm, finesse $\mathcal{F}_c = 7.71(5) \times 10^4$) and the trapping light ($\lambda_t = 937$ nm, $\mathcal{F}_t = 3.7(2) \times 10^2$). To load atoms into a small volume, so that we can cool with limited laser power (~ 3 μW) at large detuning, we initially load the atoms from a magneto-optical trap into a single-beam dipole trap formed by a 937-nm trapping beam propagating normal to the cavity mode (along \hat{x}), and focused to a waist of 2 μm . We then transfer atoms from this single-beam dipole trap to the intracavity standing-wave dipole trap. In this way, we create a small atomic cloud of about 200 atoms trapped primarily at two antinodes of the cavity standing-wave trap (along \hat{z}). The radial and axial trap vibrational frequencies are $\omega_{rad}/2\pi = 3$ kHz and $\omega_{ax}/2\pi = 350$ kHz, respectively, and the initial peak atomic density is $n_0 = 4.5 \times 10^{12}$ cm^{-3} . The typical temperature in the cavity dipole trap prior to cavity cooling is $T_i \sim 200$ μK . Since the upper hyperfine state manifold $F = 4$ of the electronic ground state $6S_{1/2}$ exhibits an unusually fast atom loss at our atomic densities [34], we continuously deplete the $F = 4$ manifold using near-resonant $6S_{1/2}$, $F = 4 \rightarrow 6P_{3/2}$, $F' = 4$ depumping

* Current affiliation: Birck Nanotechnology Center, School of Electrical and Computer Engineering, Purdue University, West Lafayette, Indiana 47907, USA

† Current affiliation: JQI and Department of Physics, University of Maryland, College Park, Maryland 20742, USA

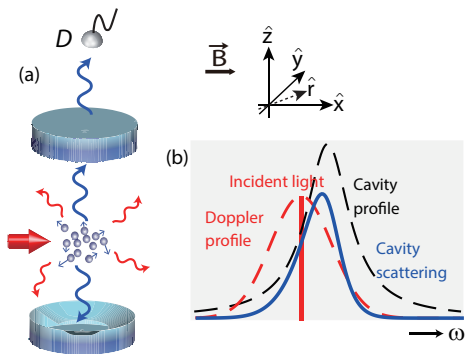


FIG. 1. (a) Schematic representation of cavity cooling of an atomic ensemble. Laser light detuned from the atomic transitions by several hundred atomic linewidths, and slightly red-detuned from the cavity resonance frequency, illuminates the atoms from the side. (b) The blue-detuned part of the Doppler-broadened atomic emission spectrum (red dashed line) is enhanced by the cavity. Thus the light scattered into the cavity (blue solid line) has an average frequency that exceeds that of the incident light (red solid line), thereby extracting thermal energy from the atoms. The final temperature is set by the cavity linewidth. Light collected from the cavity on detector D is used to measure the atomic temperature during cooling.

light. The cavity cooling light is red-detuned by several GHz from the $F = 3 \rightarrow F' = 2$ transition, horizontally polarized (along the \hat{y} direction), propagating normal to the cavity axis (along the \hat{x} direction, Fig.1(a)), and focused to a waist of $10 \mu\text{m}$ at the atoms' location. It is also red-detuned by approximately a quarter of the cavity linewidth ($|\delta_i|/2\pi \sim 40 \text{ kHz}$) from the cavity resonance, such that the cavity enhances the blue-detuned part of the atomic Doppler emission spectrum, thereby reducing the thermal energy of the atoms in the cavity scattering process (Fig.1(b)). A magnetic field along the \hat{x} axis, $B_x = 3 \text{ G}$, sets the quantization axis. The cooperativity of the cavity is given by the ratio of the single-photon Rabi frequency, $2g$, to atomic (Γ) and cavity (κ) energy decay rates, $\eta = 4g^2/\kappa\Gamma$. Due to pointing fluctuations of the single-beam dipole trap, the cooperativity varies between the maximum value of 5, averaged over hyperfine atomic transitions, at the antinodes of the cavity standing wave and the minimum value of 0 at the nodes. For the analysis below, we use the averaged value of $\eta = 2.5$. The cooperativity equals the ratio of the scattering rate into the resonant cavity to the scattering rate into free space [35].

The temperature of the atomic ensemble is sufficiently low to ensure that the Doppler width of the atoms is comparable to or smaller than the cavity linewidth. In this regime, the intensity autocorrelation function $g^{(2)}$ of the light emerging from the cavity reflects primarily the Doppler coherence time, and can be used to extract the temperature of the atomic ensemble after correcting

for the effect of the cavity linewidth (Fig.2(a)). This new method of measuring temperature is in situ and in real time, non-destructive, and can be applied to small atomic samples. (The temperature can also be measured via the spectrum of the scattered light, and the two methods agree, as detailed in the Supplemental Information.) Since the atoms are confined in the Lamb-Dicke regime along the \hat{z} direction (ω_{ax} far exceeds the recoil energy $E_{rec}/\hbar = 2\pi \times 2 \text{ kHz}$), the Doppler coherence time of the photons scattered from the incident cooling beam into the cavity is set only by the temperature along the \hat{x} direction. However, all directions thermalize quickly due to interatomic collisions on a typical timescale of 15 ms at the beginning of the cooling and 1 ms at the end of the cooling, calculated from the measured Cs elastic cross section [34]. We verify the cross thermalization by briefly applying a weak laser pulse with horizontal polarization every 3 ms with the same frequency but almost perpendicular direction (angle 75°) as the cooling beam (the \hat{r} direction in the x-y plane in Fig.1(a)). The cavity scattering from this beam measures predominantly the temperature along the \hat{y} direction, with a small (7%) contribution from the \hat{x} direction. The \hat{x} and \hat{r} measurements are distinguished by separating the near-orthogonal polarizations on two detectors. The data (inset to Fig.2(b)) show that the \hat{r} and \hat{x} directions indeed thermalize on a characteristic time below the cooling time scale of 30 ms. Note that if the atoms were not thermalizing collisionally, one could apply both beams simultaneously to cool the atoms in a horizontal plane (see S.M.), while direct axial sideband cooling along the vertical direction could be accomplished by detuning the incident frequency by the vibrational splitting ω_{ax} [14].

Fig.2(b) shows the time evolution of the atomic temperature during cooling. Starting by tuning the light onto cavity resonance and recording the $g^{(2)}$ function, we measure the initial temperature of the cloud to be about 200 μK . After tuning the input light frequency to the red of the cavity resonance (laser-cavity detuning $\delta_i/2\pi \approx -40 \text{ kHz}$) at time $t = 0$, cooling begins and the temperature drops exponentially with a time constant $\tau = 16(1) \text{ ms}$. Note that the cooling time scale varies between different data sets we present in the Letter because different incident laser powers were used. However, the final temperatures remain the same. The ensemble reaches a minimum temperature after $\sim 50 \text{ ms}$, limited by the atomic recoil and residual heating due to trap intensity fluctuations. To demonstrate that the cooling is independent of the atomic structure and depends on the light-atom detuning, Δ , only through the Δ -dependent atomic polarizability and associated photon scattering rate, we compare the cooling at $\Delta/2\pi = -2 \text{ GHz}$ and $\Delta/2\pi = -4 \text{ GHz}$ from the $F = 3 \rightarrow F' = 2$ transition. When the power is adjusted to keep the photon scattering rate the same in both cases, we observe very similar cooling performances (Fig. 2(b)), indicating that with sufficient laser power,

cavity cooling can be performed at arbitrary detuning from atomic resonance. For the remainder of the data we choose the detuning $\Delta/2\pi = -2$ GHz.

The evolution of the atomic temperature T for the cavity cooling of individual atoms can be modeled as [14]

$$\frac{dT}{dt} = -R_c\eta\Gamma_{sc}T + H_{rec}\Gamma_{sc} + h_{trap}. \quad (1)$$

Here the first term with $R_c = -\frac{16E_{rec}}{3\hbar\kappa} \frac{2\delta_i/\kappa}{[1+(2\delta_i/\kappa)^2]^2}$ describes the cavity cooling due to the scattering of light into the cavity that is blue detuned by $-\delta_i$ relative to the incident light, where $E_{rec} = \hbar^2k^2/2m$ is the recoil energy associated with the wavenumber k of the incident light, and Γ_{sc} is the photon scattering rate per atom into free space. Here it has been assumed that the Doppler width is less than the cavity linewidth κ , which for our parameters is fulfilled for $T \lesssim 300$ μK ; see Ref. [14] for the general case. The second term with $H_{rec} = \frac{4E_{rec}}{3k_B} [1 + \frac{\eta}{1+(2\delta_i/\kappa)^2}]$ describes the recoil heating associated with photon scattering both into free space and into the cavity. The third term represents the background heating due to dipole trap intensity fluctuations, which is independent of cavity cooling, and has been separately measured to be $h_{trap} = (3 \pm 1)$ $\mu\text{K}/\text{ms}$ in our system.

The final temperature T_f can be obtained by solving Eq.1 in steady state. In the limit of low trap heating and high cooperativity, the minimum temperature is reached at the cavity detuning $\delta_i = -\kappa/2$, and the final temperature is $T_f = \frac{1}{k_B} \frac{\hbar\kappa}{2} (1 + \frac{2}{\eta}) + \frac{3\hbar\kappa}{4E_{rec}\eta\Gamma_{sc}} h_{trap}$ [14]. With limited cooperativity, the minimum temperature is achieved when the laser is tuned closer to the cavity resonance. For our parameters, we find a cavity detuning $\delta_i/2\pi$ around -40 kHz to be optimal, yielding a final temperature of $T_f = 33(5)$ μK , in agreement with the predicted value of 30 μK from $h_{trap} = 2$ $\mu\text{K}/\text{ms}$.

To verify that we can approach the theoretical limit of $T_{min} = \frac{1}{k_B} \frac{\hbar\kappa}{2} (1 + \frac{2}{\eta})$ in the absence of trap heating, we reduce the trap depth U , which reduces trap heating. As Fig. 2(c) shows, we then observe further cavity cooling down to $10(1)$ μK when the trap depth U_f is reduced to 15% of its original value U_i . This is close to the predicted theoretical limit of $T_{min} = 7$ μK for ideal cavity cooling.

We also verify directly that the postulated mechanism for cavity cooling, the blue shift of the cavity-scattered light relative to the incident light, is indeed responsible for the observed cooling. By interfering the light emerging from the cavity with a local oscillator detuned by 2 MHz from the frequency of the input light, we can directly monitor the emission spectrum by the atoms into the cavity at different times during the cooling sequence (Fig.2(d)). The observed initial average blue shift of the cavity emission spectrum relative to the incident light of $\delta\omega/2\pi = 45$ kHz in combination with the observed single-atom photon scattering rate into the cavity of $\Gamma_{cav} = 6$ ms^{-1} then predicts a cooling rate constant of

$$\tau = \frac{3}{2}k_B T / \hbar\delta\omega\Gamma_{cav} = 24$$
 ms, close to the observed value $\tau_c = 17(2)$ ms.

While the temperature of the ensemble decreases, we observe some loss of atoms from light-induced collisions [36]. The atom number N , determined from the observed scattering rate into the cavity, as a function of cooling time is plotted in Fig.3(a). The loss is reasonably well described by the model for light-induced collisions [36] $\dot{N} = -\mathcal{L}\Gamma_{sc}n\lambda^3N$, where $n = n_0/2^{3/2} = 1.6 \times 10^{12}$ cm^{-3} is the average density, $\lambda = k^{-1}$ the reduced probe wavelength, and $\mathcal{L} = 0.76$ a parameter of order unity. To quantify the cooling efficiency in the presence of loss, we consider the logarithmic derivative $\gamma = -d \ln(D)/d \ln(N)$ that is used in evaporative cooling processes to characterize the cooling efficiency. Here $D = n_0\lambda_T^3$, with the peak atomic density n_0 and thermal de Broglie wavelength λ_T , is the peak phase space density. During 80 ms cooling time, the phase space density ramps up by over two orders of magnitude while one third of the atoms remain (Fig.3(b)). A fit to Fig.3(b) gives $\gamma = 5.0(3)$ whereas $\gamma = 4$ is the largest value that has been realized in evaporative cooling [37]. Furthermore, the light-induced loss could be suppressed by more than an order of magnitude by means of magnetically tuning the scattering length [38] or choosing an optimal detuning [36]. This indicates that cavity cooling is potentially an efficient method for increasing the phase space density. When we use circularly polarized cooling light to also optically pump the atoms into the magnetic sub-level $F = 3, m_F = 3$, we reach a phase space density of $D = 2(1) \times 10^{-4}$, limited primarily by the cavity linewidth.

In conclusion, we have demonstrated cavity cooling of an atomic ensemble trapped inside a high-finesse optical resonator. The results could be extended in several directions. By increasing the available laser power from 3 μW to 1 W, the detuning of the light could be increased from 4 GHz to 2 THz, comparable to typical vibrational frequency splittings in molecules, and much larger than the rotational energy splittings. Working at such large detuning makes it possible to cool different molecular rovibrational states simultaneously. Also, due to the enhancement of cavity scattering over free-space scattering by the cooperativity η , for a state-of-the-art cavity with $\eta = 200$, the cooling could be faster than the optical pumping into a different molecular state. In combination with some vibrational cooling [39], or a magneto-optical trap for molecules [40], this could allow the simultaneous cooling of molecules in many different rovibrational states [41]. With higher pump power, atomic self-organization, which could boost cooling performance, comes into play [13, 33, 42].

This work was supported by the NSF, the NSF Center for Ultracold Atoms, MURI grants through AFOSR and ARO, and NASA. Y.-T. C. acknowledges support from the Top University Strategic Alliance Fellowship.

-
- [1] R. J. Thompson, G. Rempe, and H. J. Kimble, *Phys. Rev. Lett.* **68**, 1132 (1992).
- [2] H. J. Kimble, *Physica Scripta*. **T76**, 127 (1998).
- [3] I. Fushman, D. Englund, A. Faraon, N. Stoltz, P. Petroff, and J. Vuckovic, *Science* **320**, 769 (2008).
- [4] B. Hacker, S. Welte, G. Rempe, and S. Ritter, *Nature* **536**, 193 (2016).
- [5] J. Volz, M. Scheucher, C. Junge, and A. Rauschenbeutel, *Nat. Phot.* **8**, 965 (2014).
- [6] D. W. C. Brooks, T. Botter, S. Schreppler, T. P. Purdy, N. Brahms, and D. M. Stamper-Kurn, *Nature* **488**, 476 (2012).
- [7] R. McConnell, H. Zhang, J. Hu, S. Čuk, and V. Vuletić, *Nature* **519**, 439 (2015).
- [8] O. Hosten, N. J. Engelsen, R. Krishnakumar, and M. A. Kasevich, *Nature* **529**, 505 (2016).
- [9] Z. Chen, J. G. Bohnet, S. R. Sankar, J. Dai, and J. K. Thompson, *Phys. Rev. Lett.* **106**, 133601 (2011).
- [10] P. Horak, G. Hechenblaikner, K. M. Gheri, H. Stecher, and H. Ritsch, *Phys. Rev. Lett.* **79**, 4974 (1997).
- [11] V. Vuletić and S. Chu, *Phys. Rev. Lett.* **84**, 3787 (2000).
- [12] K. Murr, S. Nußmann, T. Puppe, M. Hijkema, B. Weber, S. C. Webster, A. Kuhn, and G. Rempe, *Phys. Rev. A* **73**, 063415 (2006).
- [13] M. Xu, S. B. Jäger, S. Schütz, J. Cooper, G. Morigi, and M. J. Holland, *Phys. Rev. Lett.* **116**, 153002 (2016).
- [14] V. Vuletić, H. W. Chan, and A. T. Black, *Phys. Rev. A* **64**, 033405 (2001).
- [15] P. Maunz, T. Puppe, I. Schuster, N. Syassen, P. W. H. Pinkse, and G. Rempe, *Nature* **428**, 50 (2004).
- [16] D. R. Leibbrandt, J. Labaziewicz, V. Vuletić, and I. L. Chuang, *Phys. Rev. Lett.* **103**, 103001 (2009).
- [17] M. H. Schleier-Smith, I. D. Leroux, H. Zhang, M. A. Van Camp, and V. Vuletić, *Phys. Rev. Lett.* **107**, 143005 (2011).
- [18] M. Wolke, J. Klinner, H. Keßler, and A. Hemmerich, *Science* **337**, 75 (2012).
- [19] H. W. Chan, A. T. Black, and V. Vuletić, *Phys. Rev. Lett.* **90**, 063003 (2003).
- [20] P. Asenbaum, S. Kuhn, S. Nimmrichter, U. Sezer, and M. Arndt, *Nat. Commun.* **4**, 2743 (2013).
- [21] J. Millen, P. Z. G. Fonseca, T. Mavrogordatos, T. S. Monteiro, and P. F. Barker, *Phys. Rev. Lett.* **114**, 123602 (2015).
- [22] N. Kiesel, F. Blaser, U. Delić, D. Grass, R. Kaltenbaek, and M. Aspelmeyer, *Proc. Natl. Acad. Sci. U.S.A.* **110**, 14180 (2013).
- [23] F. Marquardt and S. Girvin, *Physics* **2**, 40 (2009).
- [24] C. H. Metzger and K. Karrai, *Nature* **432**, 1002 (2004).
- [25] T. Corbitt, Y. Chen, E. Innerhofer, H. Müller-Ebhardt, D. Ottaway, H. Rehbein, D. Sigg, S. Whitcomb, C. Wipf, and N. Mavalvala, *Phys. Rev. Lett.* **98**, 150802 (2007).
- [26] S. Gigan, H. R. Böhm, M. Paternostro, F. Blaser, G. Langer, J. B. Hertzberg, K. C. Schwab, D. Bäuerle, M. Aspelmeyer, and A. Zeilinger, *Nature* **444**, 67 (2006).
- [27] O. Arcizet, P.-F. Cohadon, T. Briant, M. Pinard, and A. Heidmann, *Nature* **444**, 71 (2006).
- [28] A. Schliesser, P. Del’Haye, N. Nooshi, K. J. Vahala, and T. J. Kippenberg, *Phys. Rev. Lett.* **97**, 243905 (2006).
- [29] J. D. Thompson, B. M. Zwickl, A. M. Jayich, F. Marquardt, S. M. Girvin, and J. G. E. Harris, *Nature* **452**, 72 (2008).
- [30] F. Marquardt, J. P. Chen, A. A. Clerk, and S. M. Girvin, *Phys. Rev. Lett.* **99**, 093902 (2007).
- [31] S. Zippilli, G. Morigi, and H. Ritsch, *EPJ D* **31**, 507 (2004).
- [32] A. Beige, P. L. Knight, and G. Vitiello, *New J. Phys.* **7**, 96 (2005).
- [33] W. Niedenzu, T. Grieser, and H. Ritsch, *EPL* **96**, 43001 (2011).
- [34] C. Chin, V. Vuletić, A. J. Kerman, and S. Chu, *Phys. Rev. Lett.* **85**, 2717 (2000).
- [35] H. Tanji-Suzuki, I. D. Leroux, M. H. Schleier-Smith, M. Cetina, A. Griera, J. Simon, and V. Vuletić, *Adv. At. Mol. Opt.* **60**, 201 (2011).
- [36] K. Burnett, P. S. Julienne, and K.-A. Suominen, *Phys. Rev. Lett.* **77**, 1416 (1996).
- [37] A. J. Olson, R. J. Niffenegger, and Y. P. Chen, *Phys. Rev. A* **87**, 053613 (2013).
- [38] V. Vuletić, C. Chin, A. J. Kerman, and S. Chu, *Phys. Rev. Lett.* **83**, 943 (1999).
- [39] M. Viteau, A. Chotia, M. Allegrini, N. Bouloufa, O. Dulieu, D. Comparat, and P. Pillet, *Science* **321**, 232 (2008).
- [40] J. Barry, D. McCarron, E. Norrgard, M. Steinecker, and D. DeMille, *Nature* **512**, 286 (2014).
- [41] B. L. Lev, A. Vukics, E. R. Hudson, B. C. Sawyer, P. Domokos, H. Ritsch, and J. Ye, *Phys. Rev. A* **77**, 023402 (2008).
- [42] S. B. Jäger, M. Xu, S. Schütz, M. J. Holland, and G. Morigi, arXiv:1702.01561.

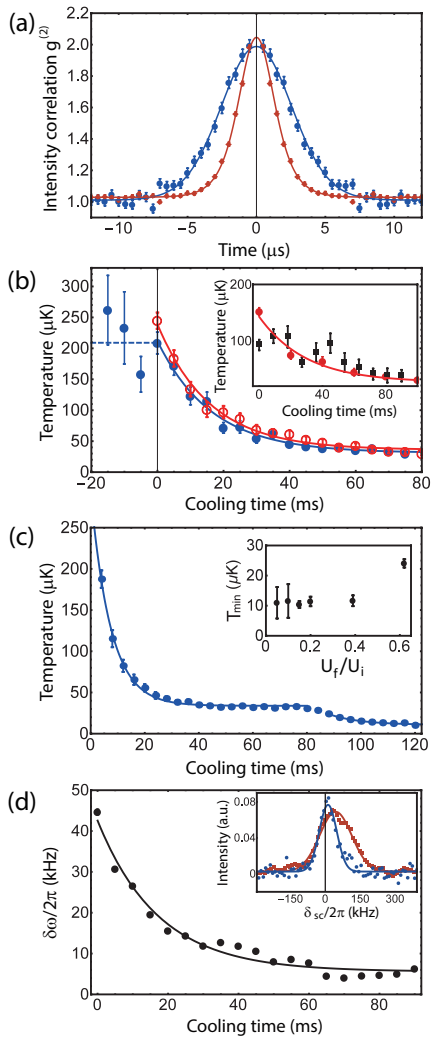


FIG. 2. (a) Photon-photon correlation function $g^{(2)}$ of the light exiting the cavity, set by the Doppler decoherence time, and used to measure the atomic temperature during cooling. $g^{(2)}$ of the scattered light is depicted for hot (red, $T = 200 \mu\text{K}$) and cold (blue, $T = 30 \mu\text{K}$) atoms. (b) Temperature as a function of cooling time for detunings $\Delta/2\pi = -2$ GHz (filled circles) and $\Delta/2\pi = -4$ GHz (empty circles) from atomic resonance extracted from $g^{(2)}$. The cooling light is tuned away from cavity resonance at $t = 0$ ms to start the cooling. The photon scattering rate per atom into the cavity $\Gamma_{cav} = 11 \text{ ms}^{-1}$ is chosen the same for both detunings. The solid lines are an exponential fits to the data with $1/e$ time of $16(1)$ ms for both detunings. The inset shows that the atomic temperatures along different directions (black squares for temperature along \hat{r} , red circles for temperature along \hat{x}) equilibrate within 30 ms. The data are taken at atomic detuning $\Delta/2\pi = -2$ GHz. (c) At time $t = 80$ ms the trap depth is reduced to 15% of its initial depth to reduce heating by trap fluctuations. In the shallower trap, the final temperature is lower and reaches $T = 10 \mu\text{K}$, i.e., $k_B T = 1.3\hbar\kappa$, close to the fundamental limit of cavity cooling. The solid lines are exponential fits for the first ($1/e$ time of $6.7(2)$ ms) and second ($1/e$ time of $11(1)$ ms) cooling stages. The inset shows the final temperature achieved as a function of the final trap depth. (d) Frequency shift $\delta\omega$ of the peak of the atomic emission spectrum into the cavity. Inset is a typical plot for the emission spectrum at the beginning (red squares, $T = 200 \mu\text{K}$) and the end (blue circles, $T = 30 \mu\text{K}$) of the cooling. δ_{sc} is the detuning from the incident light. Error bars in this and following figures are statistical errors (± 1 standard deviation).

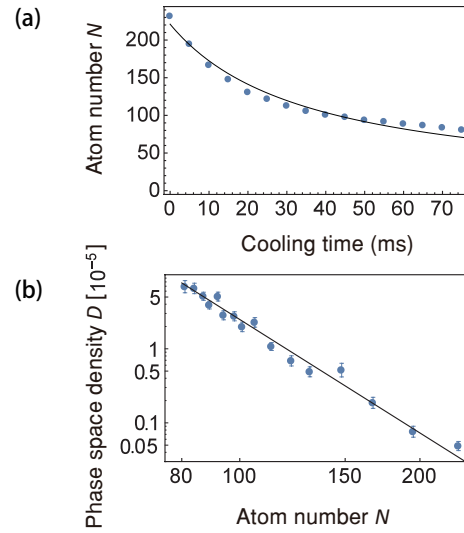


FIG. 3. (a) Atom number extracted from the total scattering rate into the cavity. The solid line is a two-body loss model fitted to the experimental data with fitted two-body loss coefficient of $0.12(1)$ $1/\text{s}$. (b) Phase space density D as a function of remaining atom number. A linear fit between $\ln(D)$ and $\ln(N)$ is plotted as a solid line. The fit gives $\gamma = 5.0(3)$.